Synthesis of Monodisperse Biotinylated p(NIPAAm)-Coated Iron Oxide Magnetic Nanoparticles and their Bioconjugation to Streptavidin

Ravin Narain,*,† Marcela Gonzales,‡ Allan S. Hoffman,*,§ Patrick S. Stayton,*,§ and Kannan M. Krishnan*,‡

Department of Chemistry and Biochemistry, Laurentian University, Sudbury, ON, P3E 2C6, Canada, Department of Material Sciences and Engineering, University of Washington, 323 Roberts Hall, Box 352120, and Department of Bioengineering, University of Washington, Foege Building, Box 355061, Seattle, Washington 98195

Received January 31, 2007. In Final Form: March 2, 2007

We describe here the synthesis of 10 nm, monodisperse, iron oxide nanoparticles that we have coated with temperature-sensitive, biotinylated p(NIPAAm) (*b*-PNIPAAm). The PNIPAAm was prepared by the reversible addition fragmentation chain transfer polymerization (RAFT), and one end was biotinylated with a PEO maleimide-activated biotin to form a stable thioether linkage. The original synthesized iron oxide particles were stabilized with oleic acid. They were dispersed in dioxane, and the oleic acid molecules were then reversibly exchanged with a mixture of PNIPAAm and *b*-PNIPAAm at 60 °C. The *b*-PNIPAAm-coated magnetic nanoparticles were found to have an average diameter of ∼15 nm by dynamic light scattering and transmission electron microscopy. The ability of the biotin terminal groups on the *b*-PNIPAAm-coated nanoparticles to interact with streptavidin was confirmed by fluorescence and surface plasmon resonance. It was found that the *b*-PNIPAAm-coated iron oxide nanoparticles can still bind with high affinity to streptavidin in solution or when the streptavidin is immobilized on a surface. We have also demonstrated that the binding of the biotin ligands on the surface of the temperature-responsive magnetic nanoparticles to streptavidin can be turned on and off as a function of temperature.

Introduction

Over the past few years, there has been increasing interest in the use of magnetic micro- and nanoparticles of different sizes, shapes, and compositions in the dynamic fields of bionanotechnology and biomedicine[1,2] Nanoparticles with a critical size below the superparamagnetic limit at room temperature[3] are preferred, as they exhibit magnetic behavior under an applied field which disappears once the field is removed. This on−off magnetic switching behavior has been applied in chemical and biological systems for magnetic separation applications. Much of this work involves the use of iron oxide (γ-Fe_2O_3 and Fe_3O_4) nanoparticles, because some formulations containing them have been approved by the FDA for in vivo applications. They are being studied for use as contrast agents for magnetic resonance imaging,[4,5] drug/gene delivery,[6] biosensors,[7] and hyperthermia treatment of cancer.[8] For such biomedical applications, in addition to the monodispersity and structural integrity of the nanoparticles, surface composition plays a crucial role. Surface modification should provide good colloidal stability, biocompatibility, and high recognition of the particle surface. An advanced approach is to functionalize the surface of the magnetic particles with a biological or chemical agent which binds to a specific target. For biocompatibility and colloidal stability reasons, a wide range of polymer-functionalized magnetic nanoparticles have been synthesized,[9−12] and in particular, PEGylated magnetic nanoparticles are the most widely studied.[13−16] PEGylated surfaces are well-known for reducing immunogenicity, nonspecific protein adsorption. Recently, phosphorylcholine-type surfactants or polymers were used to generate biocompatible and stable magnetoliposomes and magnetite nanoparticles.[17,18] In addition, lactobionic acid was also used to generate biocompatible magnetic nanoparticles.[19] These nanoparticles were found to be very promising candidates for liver diagnosis due to the very specific

* Corresponding authors. stayton@u.washington.edu, rnarain@laurentian.ca, kannanmk@u.washington.edu, or hoffman@u.washington.edu.

† Laurentian University.

‡ Department of Material Sciences and Engineering, University of Washington.

§ Department of Bioengineering, University of Washington.

(1) Gupta, A. K.; Gupta, M. *Biomaterials* **2005**, *26*, 395−4021.

(2) (a) Neuberger, T.; Schopf, B.; Hofman, H.; Hofman, M.; von Recherberg, B. *J. Magn. Magn. Mater.* **2005**, *293*, 483−496. (b) Hafeli, U.; Schutt, W.; Teller, J.; Zborowski M. *Scientific and Clinical Applications of Magnetic Carriers*; Plenum: New York, 1997.

(3) Krishnan, K. M.; Pakhomov A. B.; Bao, Y.; Blomqvist P.; Chun, Y.; Gonzales, M.; Griffin, K.; Ji, X.; Roberts, B. K. *J. Mater. Sci.* **2006**, 41, 793−815

(4) Berret, J.-F.; Schonbeck, N.; Gazeau, F.; El Kharrat, D.; Sandre, O.; Vacher, A.; Airiau, M. *J. Am. Chem. Soc.* **2006**, *128*, 1755−1761.

(5) Jun, Y.-W.; Huh, Y.-M.; Choi, J.-S.; Lee, J.-H.; Song, H.-T.; Kim, S.-J.; Yoon, S.; Kim, K.-S.; Shin, J.-S.; Suh, J.-S.; Cheon, J. *J. Am. Chem. Soc.* **2005**, *127*, 5732−5733.

(6) (a) Jain, T. K.; Morales, M. A.; Sahoo, S. K.; Leslie-Pelecky, D. L.; Labhasetwar, V. *Mol. Pharm.* **2005**, *2*, 194−205. (b) Gonzales, M.; Shapiro, E.; Koretsky A.; Krishnan, K. M. *J. Am. Chem. Soc.* Submitted for publication.

(7) Xu, C.; Xu, K.; Gu, H.; Zheng, R.; Liu, H.; Zhang, X.; Guo, Z.; Xu, B. *J. Am. Chem. Soc.* **2004**, *126*, 9938−9939.

(8) (a) Jordan, A.; Scholz, R.; Wust, P.; Schirra, H.; Schiestel, T.; Schmidt, H.; Felix, R. *J. Magn. Magn. Mater.* **1999**, *194*, 185−196. (b) Gonzales, M.; Zeisberger M.; Krishnan, K. M. *J. Appl. Phys.* In press.

(9) Kim, D. K.; Mikhaylova, M.; Zhang, Y.; Muhammed, M. *Chem. Mater.* **2003**, *15*, 1617−1627.

(10) Kim, D. K.; Mikhaylova, M.; Wang, F. H.; Kehr, J.; Bjelke, B.; Zhang, Y.; Tsakalakos, T.; Muhammed, M. *Chem. Mater.* **2003**, *15*, 4343−4351.

(11) Mikhaylova, M.; Kim, D. K.; Berry, C. C.; Zagorodni, A.; Toprak, M.; Curtis, A. S. G.; Muhammed, M. *Chem. Mater.* **2004**, *16*, 2344−2354.

(12) (a) Gupta, A. K.; Gupta, M. *Biomaterials* **2005**, *26*, 1565−1573. (b) Gonzales M.; Krishnan, K. M. *J. Magn. Magn. Mater.* In press.

(13) Thunemann, A. F.; Schutt, D.; Kaufner, L.; Pison, U.; Mohwald, H. *Langmuir* **2006**, *22*, 2351−2357.

(14) Zhang, Y.; Kohler, N.; Zhang, M. *Biomaterials* **2002**, *23*, 1553−1561.

(15) Kohler, N.; Fryxell, G. E.; Zhang, M. A. *J. Am. Chem. Soc.* **2004**, *126*, 7206−7211.

(16) Veiseh, O.; Sun, C.; Gunn, J.; Kohler, N.; Gabikian, P.; Lee, D.; Bhattarai, N.; Ellenbogen, R.; Sze, R.; Hallahan, A.; Olson, J.; Zhang, M. *Nano Lett.* **2005**, *5*, 1003−1008.

(17) Hu, F.; Neoh, K. G.; Cen, L.; Kang, E.-T. *Biomacromolecules* **2006**, *7*, 809−816.

(18) (a) Yuan, J.-J.; Armes, S. P.; Takabayashi, Y.; Prassides, K.; Leite C. A. P.; Galembeck F.; Lewis A. L. *Langmuir* **2006**, *22*, 10989−10993. (b) Gonzales, M.; Krishnan, K. M. *J. Magn. Magn. Mater.* **2005**, *293*, 265−270.

10.1021/la700268g CCC: $37.00
Published on Web 04/24/2007

interaction of the galactose residue to hepatocytes. Herein, we report the synthesis of colloidally stable biotinylated p(*N*-isopropylacrylamide) surface coated, monodisperse iron oxide nanoparticles. Magnetic thermoresponsive core−shell nanoparticles and microparticles have previously been reported and have been applied to several biorelated applications.[20−24] These functionalized magnetic nanoparticles are temperature-sensitive and have a biotin ligand conjugated to their surface. The ligand coating can potentially specifically bind to the streptavidin protein as a function of temperature. A series of telechelic PNIPAAm was synthesized via the reversible addition fragmentation chain transfer polymerization (RAFT).[25] PNIPAAm, with target degree of polymerization of 200, was selected to generate the functionalized magnetite nanoparticles.

Experimental Section

Materials. All chemicals were purchased from Sigma-Aldrich, Acros, or Pierce Chemicals and were used as received unless otherwise stated. *N*-Isopropylacrylamide (NIPAAm) was recrystallized from hexane prior to use.

Characterization. Molecular weights and molecular weight distributions were assessed by gel permeation chromatography (GPC) using an organic eluent. The following protocols were used in this work. The polymers were analyzed using a Viscotek GPC instrument. The system comprises a dual detector (refractive index detector and viscometer) and mixed Viscogel columns, and DMF containing 0.1 M LiBr was used as the eluent at a flow rate of 1.0 mL min^{-1}. Calibration was achieved using a series of monodisperse polystyrene standards. The molecular weights and polydispersity data were calculated using the OmniSEC software package. ^1H and ^{13}C NMR spectra were recorded on a 200 MHz Varian spectrometer. Cloud points of PNIPAAm and PNIPAAm-coated iron oxide magnetite nanoparticles were obtained using a thermoregulated Cary 100 Bio UV-visible spectrophotometer coupled to a temperature controller in the absorbance mode at a wavelength of 380 nm and a heating rate of 0.5 °C/min.

Dynamic light scattering experiments were performed on a Viscotek DLS instrument containing a He−Ne laser at a wavelength of 632 nm and a Pelletier heater.

Fluorescence Measurements. All fluorescence measurement data were obtained using a Shimadzu Fluorimeter. Displaced fluorescein−biotin was measured at an excitation wavelength of 492 nm and an emission wavelength of 510 nm.

Surface Plasmon Resonance Measurements. A Biacore X SPR was used to study the binding events between the biotinylated magnetic nanoparticles and the surface-immobilized streptavidin sensor chip. The buffer (HEPES - 0.01 M, 0.15 M NaCl, 0.005% surfactant P20) and SA-coated sensor chip were purchased from Biacore Inc. The flow rate was set to 10 μL/min, and between 25 and 50 μL of sample was injected at a time.

Preparation of Poly(*N*-isopropylacrylamide) by Reversible Addition−Fragmentation Chain Transfer Polymerization (RAFT). *Typical Synthesis of PNIPAAm by the RAFT Process.* *N*-Isopropylacrylamide (2.0 g, 18 mmol, target $DP_n = 200$) was dissolved in 5 mL of degassed dioxane. 4,4′-Azobis(4-cyanovaleric acid) (3 mg, 13 μmol) and *S*,*S*′-bis (α,α′-dimethyl-α″-acetic acid)-trithiocarbonate (14 mg, 50 μmol) were added, and the solution was then purged with nitrogen. The tube was sealed, and the polymerization reaction was carried out at a temperature of 60 °C for 24 h. The viscous polymer solution was cooled to room temperature and then diluted with distilled deionized water. The polymer solution was dialyzed for 48 h using a dialysis membrane of molecular weight cutoff (MWCO) of 3400. The water was changed after every 6 h for this dialysis. The polymer was then freeze-dried overnight. A flaky creamy white solid was then recovered.

Synthesis of Surfactant−Iron Oxide Nanoparticles. *Typical Synthesis of Spherical 10 nm Surfactant-Coated Iron Oxide Nanoparticles Using the Thermal Decomposition of Organometallics Method.*[26] Oleic acid (1.47 g) in 10 mL octyl ether was heated to 100 °C in an argon atmosphere. Iron pentacarbonyl (0.5 mL) was injected into the hot solution and allowed to reflux at 283 °C. After approximately 30 min, nanoparticle nucleation occurred and was evident by a sharp darkening of the solution over a 30 s period. After nucleation, the solution was allowed to reflux for an additional 1.5 h. The solution was cooled to room temperature and trimethylamine *N*-oxide added. The temperature of the solution was increased to 130 °C and heated for 2 h during which time the color of the solution turned from black to red. Afterward, the temperature was increased and allowed to reflux for 1 h during which time the color of the solution turned black. The solution was cooled to room temperature, washed with ethanol, and centrifuged to collect a black precipitate from solution.

A Phillips 420 transition electron microscope (TEM), operating at an accelerating voltage of 120 keV, and a FEI Technai scanning transmission electron microscope (STEM) (Nano-Imaging Facility, Simon Fraser University) were used to characterize nanoparticle size and shape. Ten nanometer iron oxide particles were shown to be magnetite (Fe_3O_4) by comparing the ratios of L3 to L2 transitions in electron energy-loss spectroscopy.[27]

Exchange of Surfactant on Iron Oxide with a Mixture of PNIPAAm and *b*-NIPAAm. A mixture of PNIPAAm (80 mg, $M_n \approx 22$ kDa) and *b*-PNIPAAm (20 mg, $M_n \approx 22$ kDa) was first dissolved in dioxane (20 mL), followed by the addition of surfactant (oleic acid) coated magnetite nanoparticles (20 mg). The exchange was conducted in dioxane, as PNIPAAm is insoluble in dichlorobenzene. The container was sealed, and the brownish solution was stirred at 60 °C for 48 h. Then, the dioxane was evaporated off, and the brownish solid was washed thoroughly with hexane to remove the surfactant. The brown solid was dissolved in water and dialyzed against water using a dialysis membrane of MW cutoff of 40 000 for 48 h. The solution was then lyophilized to recover 38 mg of PNIPAAm-functionalized magnetic nanoparticles.

Biotinylation of PNIPAAm. PNIPAAm ($M_n = 22\,000$ g/mol, $M_w/M_n = 1.24$) (200 mg, 9.1 μM) was first dissolved in 2 mL of *N*,*N*′-dimethylformamide (DMF), followed by the in situ addition of sodium borohydride (10 mg) and a PEO maleimide-activated biotin (Pierce) (10 mg, 18 μM). The sodium borohydride cleaves the trithioester to thiol, and the latter then reacts in situ to the PEO maleimide-activated biotin to form a stable thioether linkage. The reaction mixture was stirred for 24 h. The solution was then mixed with 5 mL of distilled deionized water and dialyzed against water for 48 h using a membrane of molecular weight cutoff of 3400. The resulting solution was then lyophilized.

HABA Assay. To determine the extent of biotinylation of PNIPAAm, the neutravidin-HABA dye (HABA: 2-hydroxyazobenzene-40-carboxylic acid) assay was used. A similar procedure reported by Lackey et al.[28] was used to check the biotin. The results demonstrate that the extent of biotinylation PNIPAAm was only 72%.

(19) Selim, K. M. K.; Ha, Y.-s.; Kim, S.-J.; Chang, Y.; Kim, T.-J.; Lee, G. H.; Kang, I.-K. *Biomaterials* **2007**, *28*, 710−716.
(20) Deng, Y.; Yang, W.; Wang, C.; Fu, S. *Adv. Mater.* **2003**, *15*, 1729.
(21) Wakamatsu, H.; Yamamoto, K.; Nakao, A.; Aoyagi, T. *J. Magn. Magn. Mater.* **2006**, *302*, 327−333.
(22) Lin C. L.; Chiu, W.-Y.; Don, T.-M. *J. Appl. Polym. Sci.* **2006**, *100*, 3987−3996.
(23) Gelbrich, T.; Feyen, M.; Schmidt, A. M. *Macromolecules* **2006**, *39*, 3469−3472.
(24) Pich, A.; Bhattacharya, S.; Lu, Y.; Boyko, V.; Adler, H.-J. P. *Langmuir* **2004**, *20*, 10708−10711.
(25) Le, T. P.; Moad, G.; Rizzardo, E.; Thang, S. H. PCT Int. Appl WO9801478 A1 980115. *Chem. Abstr.* **1998**, *128*, 115390.
(26) (a) Hyeon, T.; Lee, S. S.; Park, J.; Chung, Y.; Na, H. B. *J. Am Chem. Soc.* **2001**, *123*, 12798. (b) Gonzales, M.; Krishnan K. M *J. Magn. Magn. Mater.* ***2005***, 293, 265.
(27) Gonzales, M.; Calderon, H.; Krishnan, K. M. 2005, unpublished.
(28) Lackey, C. A.; Murthy, N.; Long, C. J.; Hayashi, Y.; Bulmus, E. V.; Hoffman, A. S.; Stayton, P. S. *Bioconjugate Chem.* **1999**, *10*, 401−405.

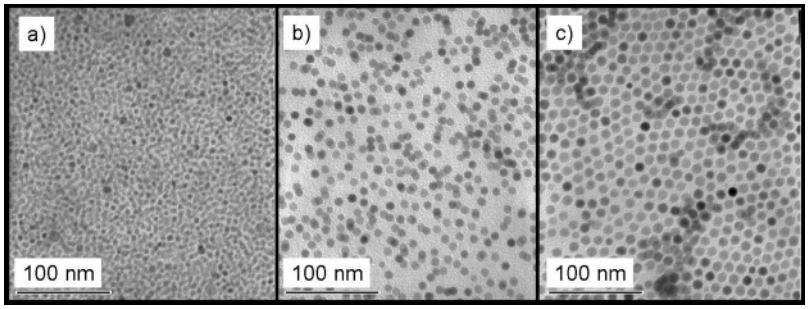

Figure 1. Transmission electron micrograph of (a) 5 nm, (b) 7 nm, and (c) 10 nm surfactant−iron oxide nanoparticles (solvent, dichlorobenzene; grid, carbon-coated copper grid).

Scheme 1. Homopolymerization of *N*-Isopropylacrylamide (NIPAAm) by the RAFT Process

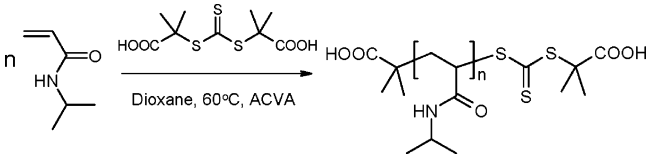

Results and Discussion

Iron oxide is the most widely accepted nanoparticle material for biological application, as it is approved for use by the Food and Drug Administration in applications such as MRI contrast enhancement. Nanoparticles made from the thermal decomposition of organometallics are extremely uniform in size, crystallinity, and shape. Control of nanoparticle size is shown in Figure 1 and achieved by adjusting the molar ratio of oleic acid to iron pentacarbonyl precursors (herein described as a 3:1 molar ratio of oleic acid to iron pentacarbonyl). The high quality of these iron oxide nanoparticles is ideal for many biological applications, as their magnetic properties are enhanced. Therefore, they may require lower dosages than particles made from other applications. However, these nanoparticles are not dispersible in aqueous solutions, and their surfactant-coated surface must first be modified[12b] prior to use in biomedical applications.

Poly(*N*-isopropylacrylamide) or PNIPAAm is one of the most studied temperature-sensitive polymers. It is well-established that PNIPAAm in aqueous solution exhibits a sharp phase transition, called the lower critical solution temperature (LCST), in the range 25−35 °C depending on aqueous solution composition. For low molecular weight PNIPAAm, it has been shown recently that the LCST can be shifted depending on the nature of the end groups.[29] PNIPAAm were prepared via reversible addition fragmentation chain transfer polymerization (RAFT) using the chain transfer agent (**CTA1**: *S*,*S*′-bis(α,α′-dimethyl-α″-acetic acid)trithiocarbonate) and 4,4′-azobis(4-cyanovaleric acid) as the initiator. The RAFT polymerization technique was chosen for two reasons: (a) it has been used previously to generate well-defined PNIPAAm having a range of molecular weights, and (b) the corresponding CTA and initiator were selected to generate telechelic PNIPAAm having a carboxylic group at one end and potentially a thiol functional group at the other end. The polymerization was carried out in dioxane under inert atmosphere (Scheme 1). The RAFT agent, **CTA1**, used in this work was first reported by Lai et al.[30] for the polymerization of a range of acrylates and methacrylates. Several research groups[31−37] have then reported the polymerization of NIPAAm and other acrylamido monomers by the RAFT process. The aqueous solution properties of the PNIPAAm were studied by UV−vis as a function of temperature and concentration. The LCST of the PNIPAAm was found to be dependent on the concentration and varies between 34 and 37 °C.

Part of the synthesized PNIPAAm ($DP_n = 200$; $M_n = 22$ kDa) was biotinylated at one end of the polymer chain. The trithiocarbonate was first cleaved by sodium borohydride in *N*,*N*′-dimethylformamide to generate the thiol functional group, followed by the in situ reaction with a PEO maleimide-activated biotin to form a thioether linkage (the reaction was done in situ to minimize the formation of disulfide linkages). The extent of biotinylation of the PNIPAAm was assessed using a 2-hydroxyazobenzene-4-carboxylic acid (HABA) assay, and 72% biotinylation of the PNIPAAm was achieved by this method. It was not obvious to determine the extent of biotinylation by ^{1}H NMR due to the overlapping of signals. The surfactant on the iron oxide nanoparticles was then exchanged at 60 °C in dioxane with a mixture of PNIPAAm (80% w/w) and biotin−PNIPAAm (20% w/w) (Scheme 2). At this temperature, the surfactant carboxylate groups attached to the surface of the magnetic nanoparticles become labile and are easily exchanged with an excess of PNIPAAm. Below 60 °C, the polymer chains are tightly bound to the surface of the magnetite nanoparticles and do not desorb when dispersed in different solvents. The PNIPAAm-coated iron oxide nanoparticles were then dispersed in THF and water. The successful dispersion of the PNIPAAm-coated iron oxide nanoparticles in water is also indicative of successful surface modification.

Dynamic light scattering (DLS) and transmission electron microscopy indicate that the nanoparticles are uniform and monodisperse and have an average diameter of ∼15 nm when dispersed in THF (Figure 2). However, the nanoparticles tend to form larger aggregates in aqueous solution (at room temperature of 25 °C) with a diameter of ∼60 nm as revealed by DLS measurements. The aggregation behavior of the temperature-sensitive biotinylated PNIPAAm magnetic nanoparticles in aqueous solution was further studied by UV−vis as a function of temperature. The thermoresponsive magnetic nanoparticles show a sharp phase transition at 32 °C (wavelength 400 nm) characteristic of PNIPAAm lower critical solution temperature (LCST).

(29) (a) Xia, Y.; Burke, N. A. D.; Stover, H. A. H. *Macromolecules* **2006**, 39, 2275. (b) Xia, Y.; Yin, X.; Burke, N. A. D.; Stover, H. A. H. *Macromolecules* **2005**, *38*, 5937−5943. (c) Housni, A.; Narain R. 2006, unpublished.

(30) Lai, J. T.; Filla, D.; Shea, R. *Macromolecules* **2002**, *35*, 6754−6756.

(31) Moad, G.; Rizzardo, E.; Thang, S. H. *Aust. J. Chem.* **2005**, *58*, 379.

(32) Convertine, A. J.; Ayres, N.; Scales, C. W.; Lowe, A. B.; McCormick, C. L. *Biomacromolecules* **2004**, *5*, 1177−1180.

(33) Convertine, A. J; Lokitz B. S.; Vasileva Y.; Myrick L. J.; Scales C. W.; Lowe A. B.; McCormick C. L. *Macromolecules* **2006**, *39*, 1724−1730.

(34) Ganachaud, F.; Monteiro, M. J.; Gilbert, R. G.; Dourges, M.-A.; Thang, S. H.; Rizzardo, E. *Macromolecules* **2000**, *33*, 6738−6745.

(35) Schilli, C.; Lanzendoerfer, M. G.; Mueller, A. H. E. *Macromolecules* **2002**, *35*, 6819−6827.

(36) Ray, B.; Isobe, Y.; Morioka, K.; Habaue, S.; Okamoto, Y.; Kamigaito, M.; Sawamoto, M. *Macromolecules* **2003**, *36*, 543−545.

(37) Yin, X.; Hoffman, A. S.; Stayton, P. S. *Biomacromolecules* **2006**, *7*, 1382.

Scheme 2. Exchange of the Surfactant with a Mixture of PNIPAAm and *b*-PNIPAAm in Dioxane on the Iron Oxide Nanoparticles at 60 °C

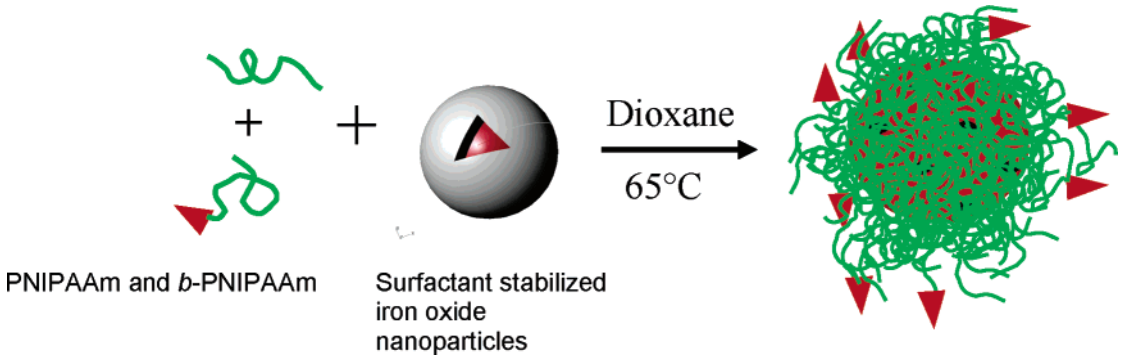

Streptavidin has four subunits and can potentially bind biotinylated PNIPAAm-coated iron oxide nanoparticles with very high affinity. It is also one of the most widely used proteins in affinity separations, bioassays, and clinical diagnostics because of its high affinity to biotin. The binding of the biotinylated PNIPAAm-coated iron oxide nanoparticles to streptavidin in aqueous solution was studied using dynamic light scattering and transmission electron microscopy. The addition of streptavidin to an aqueous dispersion of the *b*-PNIPAAm magnetic nanoparticles resulted in the formation of larger aggregates as revealed by DLS measurements (average diameter of the aggregates ~110 nm). As expected, the distribution of the aggregated nanoparticles was found to be rather polydisperse. The aggregated magnetic nanoparticles were imaged with TEM (see Figure 3). The micrographs show clearly the surface-coated magnetic nanoparticles and some aggregation of the nanoparticles caused by the streptavidin.

The motivation for biotinylation of the thermoresponsive magnetic nanoparticles is to demonstrate the feasibility of the bioactive groups on the nanoparticles toward bioconjugation to a high-affinity ligand such as streptavidin both in solution and when immobilized on a surface. The availability of the biotin as a function of temperature is also studied. The biotinylated PNIPAAm-coated iron oxide magnetic nanoparticles were first used in a displacement assay using a mutant streptavidin. A high off-rate mutant-type streptavidin protein (S45A) was used in

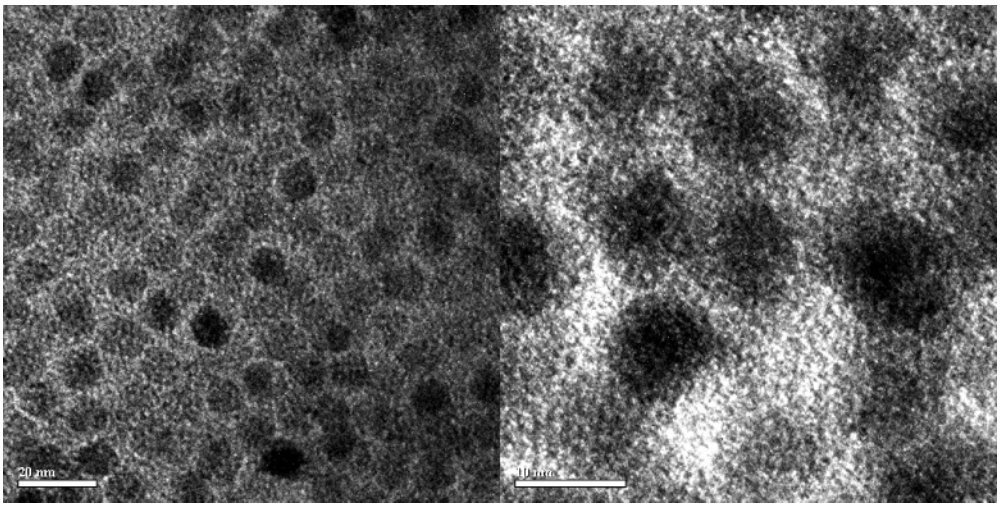

Figure 2. Transmission electron micrographs of *b*-PNIPAAm surface-coated iron oxide nanoparticles (solvent, THF; grid, carbon-coated copper grid).

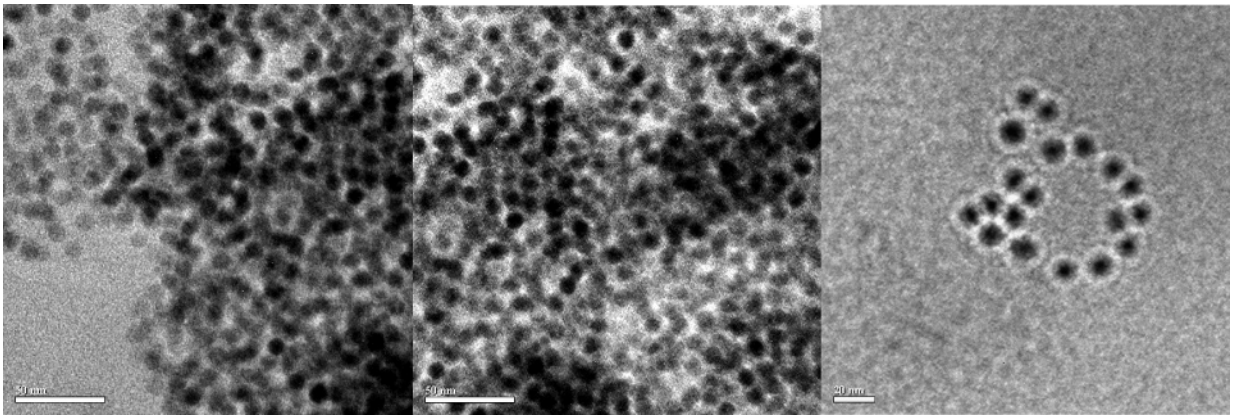

Figure 3. Transmission electron micrographs of the aggregated *b*-PNIPAAm surface-coated iron oxide nanoparticles with streptavidin (SA) (solvent, distilled deionized water; grid, carbon-coated copper grid).

Scheme 3. Schematic Representation for the Kinetic Displacement of Bound Fluorescein−Biotin on Mutant S45A with *b*-PNIPAAm Magnetite Nanoparticles

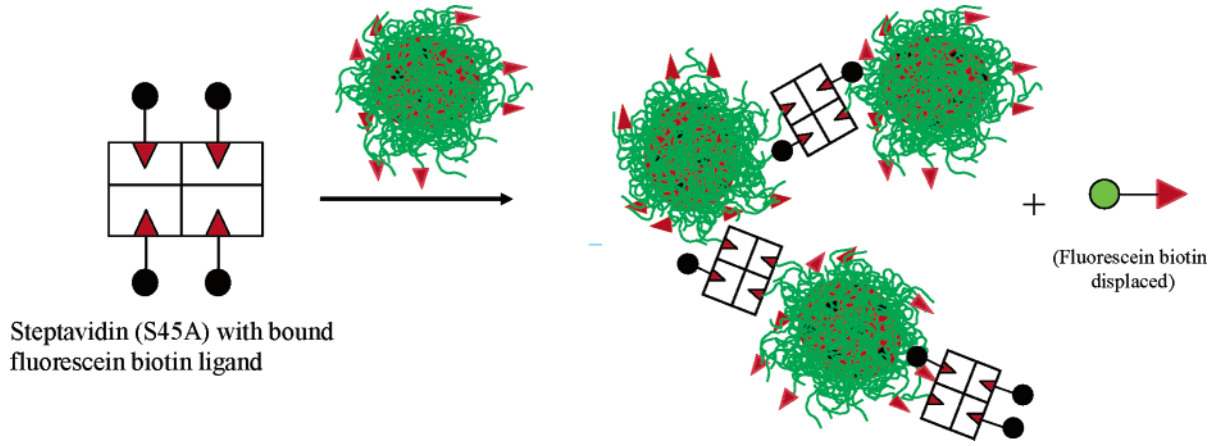

this study where bound biotin could competitively be exchanged with either an excess of free biotin or *b*-PNIPAAm or *b*-PNIPAAm surface-coated magnetic nanoparticles within minutes. Wild-type streptavidin has a much lower exchange rate with excess biotin. The four binding sites of mutant streptavidin (S45A) were first blocked with an excess fluorescein−biotin and subsequently purified to remove any residual fluorescein−biotin. The quenched and bound fluorescein−biotin on S45A was then competitively displaced with an excess of either D-biotin or *b*-PNIPAAm or *b*-PNIPAAm iron oxide nanoparticles (Scheme 3). The kinetic displacement of the bound fluorescein biotin was monitored by fluorescence spectroscopy (see Figure 4). The fluorescence measurements have shown that the displacement of the bound fluorescein−biotin at 25 °C is slow with *b*-PNIPAAm and much slower with the *b*-PNIPAAm surface-coated iron oxide nanoparticles as compared to free D-biotin. As expected, it was found that the *b*-PNIPAAm reaches a maximum similar to that of D-biotin. The displacement of the bound fluorescein biotin with the *b*-PNIPAAm and *b*-PNIPAAm iron oxide nanoparticles was also monitored as a function of temperature. Above the LCST (35 °C), the pNIPAAm chains are dehydrated and collapsed. The displacement of the surface-bound fluorescein biotin on streptavidin was found to be very slow at 35 °C. As shown in Figure 4, almost no change of fluorescence was noted at 35 °C with the *b*-PNIPAAm surface-coated iron oxide nanoparticles. At the same temperature, a very slow exchange of *b*-PNIPAAm with the bound fluorescein biotin was noted. It should be pointed out that the surface-bound fluorescein biotin on streptavidin is not affected at 35 °C, as no increase in fluorescence was observed within the 1 h experimental time. These data lead to the conclusion that, below the LCST of p(NIPAAm), the biotin ligands of the magnetic nanoparticles are still accessible for bioconjugation to streptavidin. Furthermore, we demonstrate that the biotin ligand is sterically hindered when the p(NIPAAm) chain are collapsed (above LCST). Therefore, the responsiveness of the p(NIPAAm) chain on the magnetic nanoparticles can play an important role on the rate and extent of binding of the biotin ligand to streptavidin. Similarly, we have recently shown that different molecular weights of biotinylated glycopolymers can play a crucial role in the extent of biotin binding to streptavidin.[38]

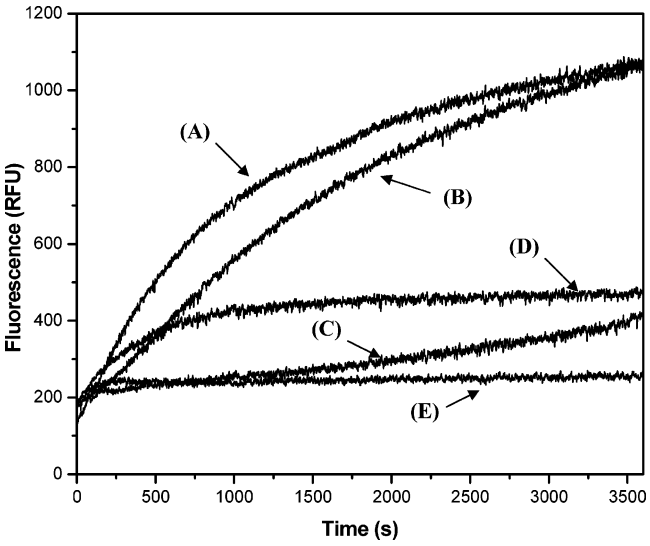

Figure 4. Fluorescence trace for the kinetic displacement of bound fluorescein−biotin from mutant streptavidin protein (S45A) in a PBS buffer with an excess of (i) D-biotin at 25 °C (A); (ii) *b*-PNIPAAm at 25 °C (B); (iii) *b*-PNIPAAm at 35 °C (C); (iv) *b*-PNIPAAm iron oxide nanoparticles at 25 °C (D); (v) *b*-PNIPAAm iron oxide nanoparticles at 35 °C (E).

The availability of the biotin on the iron oxide nanoparticles for conjugation to surface-bound streptavidin was further investigated using surface plasmon resonance (SPR) (see Figure 5). SPR is a very sensitive technique to study biomolecular events in the nanomolar range. SPR has been extensively used to study the binding events between biotinylated molecules or macromolecules to streptavidin, as the affinity of biotin to streptavidin is very strong.[39] The biotinylated iron oxide nanoparticles were injected into the SPR instrument containing a preloaded streptavidin-coated sensor chip. After injection, an immediate change in response was observed, and after automatic wash (with buffer), the difference in response is indicative of the binding of the biotinylated PNIPAAm iron oxide nanoparticles to the streptavidin on the sensor chip. After that, a solution of bovine serum albumin (BSA) was injected to ensure no nonspecific binding of the iron oxide nanoparticles. As a blank, non-biotinylated PNIPAAm and non-biotinylated PNIPAAm iron oxide nanoparticles were injected to confirm that the binding is due specifically to the biotin ligand and not to nonspecific binding of the polymer or the metal nanoparticles on the sensor chip. These results clearly show that the biotin on the magnetic nanoparticles can bind with high affinity to immobilized streptavidin.

(38) Narain, R. *React. Funct. Polym.* **2006**, *66*, 1589−1595.
(39) Vazquez-Dorbatt, V.; Maynard, H. D. *Biomacromolecules* **2006**, *7*, 2297−2302.

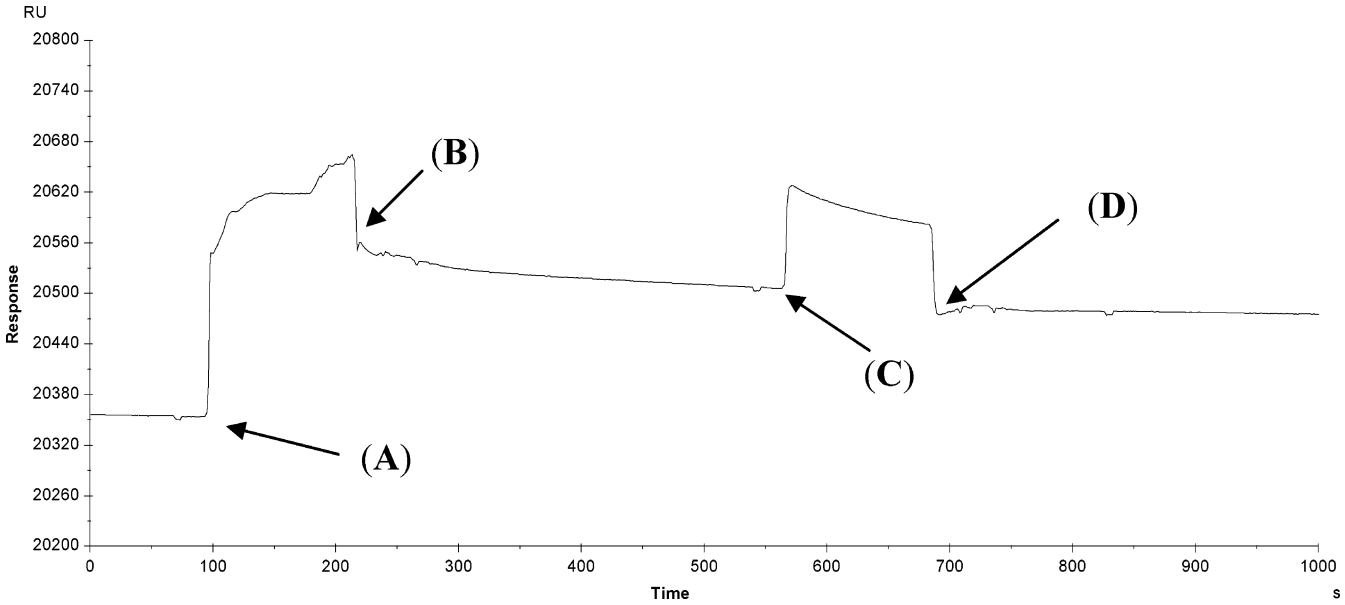

Figure 5. SPR sensorgram for the bioconjugation of the *b*-PNIPAAm surface-coated nanoparticles to streptavidin-coated sensor chip: response after sample injection and response after BSA injection (data obtained from a Biacore X instrument using HBS-EP buffer at a flow rte of 10 μL/min and temperature set at 25 °C. (A) *b*-PNIPAAm-coated iron oxide nanoparticles injection. (B) Response after wash with buffer. (C) BSA injection. (D) Final response after wash with buffer.

Conclusions

We report here the successful surface functionalization of monodisperse iron oxide nanoparticles with controlled molecular weight PNIPAAm polymer chains, initially prepared by the reversible addition−fragmentation chain transfer polymerization (RAFT). This produced a PNIPAAm molecule with a carboxylic group at one end and a thiol group at the other end. Biotin was then conjugated to the end with the thiol group, and a mixture of *b*-PNIPAAm and PNIPAAm was then used to displace the oleic acid surfactant on the magnetic nanoparticles, yielding *b*-PNIPAAm-coated iron oxide nanoparticles. The biotinylated PNIPAAm surface-coated iron oxide nanoparticles were found to be uniform and monodisperse, as revealed by the transmission electron microscopy and dynamic light scattering. The ability of the biotin on the nanoparticle surface to bind to streptavidin was monitored by fluorescence as a function of temperature, and it was found the multivalent streptavidin aggregated the *b*-PNIPAAm-coated particles. Biotin binding is drastically reduced by the collapse of the PNIPAAm chain above the lower critical solution temperature of the polymer. The availability of the biotin on the iron oxide nanoparticles for binding to surface-immobilized streptavidin was further investigated using the surface plasmon resonance technique. It was also found that the biotinylated PNIPAAm-coated iron oxide nanoparticles can still bind to the surface of a streptavidin-coated sensor chip with high affinity.

Acknowledgment. This work was partially supported by NIH grant EB000252, NSF grants DMR-0203069, DMR-0501421 the Campbell Endowment at UW, the National Physical Science Consortium, and the Natural Sciences and Engineering Research Council of Canada (NSERC).

LA700268G